OPEN

PRS GLOBAL OPEN

ORIGINAL ARTICLE
Craniofacial/Pediatric

Assessment and Identification of Improvement Areas for Facial Symmetry in Hemifacial Microsomia (Type IIB) Using Three-dimensional Measurements

Yoichiro Niikura, DDS*
Takenobu Ishii, DDS, PhD*†
Yoshiaki Sakamoto, MD, PhD‡
Dai Ariizumi, DDS, PhD*
Teruo Sakamoto, DDS, PhD†
Kenji Sueishi, DDS, PhD*

Background: Surgical planning for hemifacial microsomia (HFM) patients often involves planning the amount of maxillary movement and mandibular bone distraction from three-dimensional (3D) volumetric images constructed from computed tomography scans. By representing anatomical indicators for facial symmetry in X, Y, and Z coordinates, we identified the more challenging areas in correcting facial asymmetry.

Methods: The study included five HFM patients with a mean age of 22.2 years, all diagnosed with HFM (type IIB). We established measurement points with high reproducible 3D coordinates on the 3D volumetric images obtained from computed tomography scans for before surgery, treatment objectives, and after surgery. We assessed the symmetry of measurement points between the affected side and nonaffected side at each time point.

Results: In the before-surgery group, significant differences were observed between the affected side and nonaffected side in X,Y (excluding Palatine foramen, upper molar, canine) and Z coordinates for measurement items. In the treatment objectives group, no differences were observed between the affected side and nonaffected side in X, Y, and Z coordinates, resulting in facial symmetry. In the after-surgery group, significant differences were observed in Y coordinates in the mental foramen area, and significant differences were observed in z axis measurement items in the canine and mental foramen areas.

Conclusions: It is evident that relying solely on a front view assessment is insufficient to achieve facial symmetry. Particularly, both anterior–posterior and vertical improvements in the area near the mental foramen on the affected side are necessary.
(Plast Reconstr Surg Glob Open 2024; 12:e5877; doi: 10.1097/GOX.0000000000005877; Published online 10 June 2024.)

INTRODUCTION

Hemifacial microsomia (HFM) is a congenital condition characterized by maxillofacial skeletal structure and soft tissue underdevelopment from the first and second branchial arches with mainly facial asymmetry and microtia.[1] Among maxillofacial congenital abnormalities, it ranks second after cleft lip and palate.[2] Clinical signs include facial asymmetry due to unilateral mandible underdevelopment, whereas intraoral findings include crossbite, crowding, tilting of the occlusal plane, and dental midline deviation with the face.[3]

Treatment typically involves pre/postoperative orthodontic treatment with bone-cutting and repositioning.[4] Its diagnosis and treatment planning involves frontal and lateral cephalograms of the head. Discovered by Hofrath[5] and Broadbent[6] in 1931 with various evaluation methods established after, cephalograms are a standard assessment technique in plastic surgery, orthodontics, and craniofacial surgery. However, their three-dimensional (3D) assessments can be challenging to apply in cases with external auditory canal underdevelopment.[7] Meanwhile, advancements in computed tomography (CT) imaging precision have enabled detailed 3D reconstruction images with usable data.[8,9] Image analysis techniques have also progressed, with surgical

*From the *Department of Orthodontics, Tokyo Dental College, Tokyo, Japan; †Department of Orthodontics, Tokyo Dental College Chiba Dental Centre, Chiba, Japan; and ‡Department of Plastic and Reconstructive Surgery, Keio University School of Medicine, Tokyo, Japan.*

Received for publication January 8, 2024; accepted April 17, 2024.

DOI: 10.1097/GOX.0000000000005877

Disclosure statements are at the end of this article, following the correspondence information.

simulations using computer-aided design and computer-aided manufacturing via 3D volumetric reconstruction images.[10] However, many assessments rely on measurements of volume, distance, and angles,[11,12] including evaluations from a frontal view.[13]

With reconstructing occlusion, orthodontic, plastic, and oral surgery treatment goals need to be considered. 3D volumetric reconstruction images were created using CT for HFM patients under Le Fort I osteotomy of the maxilla and 3D bone distraction[14] of the affected side of the mandible. These images were used to express anatomical indicators for facial symmetry as X, Y, and Z coordinates to compare 3D coordinates between the affected and nonaffected sides presurgery, treatment objectives, and postsurgery. The objective of this study was to determine the 3D symmetry of the upper/lower jaw areas and assist in developing better surgical treatment strategies for HFM.

Takeaways

Question: This study used three-dimensional volume images from CT scans to assess facial asymmetry in hemifacial microsomia (HFM) patients before and after treatment using three-dimensional coordinates.

Findings: Preoperative scans showed asymmetry in X, Y (except certain dental points), and Z coordinates. Post-treatment scans achieved overall symmetry, but the mental foramen area showed insufficient improvement in Y and Z coordinates.

Meaning: These findings highlight that a front view assessment alone is inadequate for achieving facial symmetry in HFM treatment, emphasizing the need for anterior-posterior and vertical improvements near the mental foramen on the affected side.

MATERIAL AND METHODS

Subject

The criteria for the study included patients diagnosed with HFM (type IIB)[15] at Keio University Hospital's department of plastic and reconstructive surgery. Patients selected had completed their maxillofacial growth and undergone surgical orthodontic treatment. They had undergone maxillary repositioning with Le Fort I osteotomy, followed by mandibular bone distraction on the affected side and vertical ramus osteotomy on the nonaffected side. The extender has the feature of 3D movement at its tip along with maxillomandibular fixation to induce the desired occlusion. The bone distraction began one week after the bone-cutting and continued until the target was achieved with 6–12 months of stabilization.[14] Five patients (three men and two women), average age 22.2 years (19–28), were featured. CT data and medical records used for diagnosis one month pre/postsurgery were used for these patients.

This study was approved by the ethics committee of Tokyo Dental College (approval no.: 731) and the ethics committee of Keio University (approval no.: 20160207).

Preparation for 3D Measurement

CT was performed using LightSpeed 16 (GE Healthcare, Milwaukee, Wisc.), BrightSpeed S (GE Healthcare), and Discovery CT750 HD (GE Healthcare) CT scanners at the following settings: 120 kV; 70–300 mA; slice thickness, 0.625 mm; and field of view, 25 cm. CT data for each patient minus names and identification numbers were saved in DICOM format at Keio University Hospital and converted to stereolithography data using 3D structural analysis software (TRI/3D-BON version 9.0; RATOC System Engineering, Tokyo, Japan) at Tokyo Dental College (Fig. 1). A coordinate system centered on the hypophyseal fossa was prepared for each patient using 3D measurement point data processing software (Imageware version 13.2; Siemens AG, Munich, Germany), and the 3D coordinates of arbitrary points were measured. The measurement points were set as follows: In the maxilla, they included the anterior nasal spine (ANS), posterior nasal spine (PNS), greater palatine foramen (palatine foramen), the mesial buccal cusp of the first molar (upper molar), the tip of the canine (canine), and the mesial edge of the upper central incisor (upper central incisor). In the mandible, they included the center of the hole where the mental nerve exits (mental foramen), the center of the small process found in the hole where the mandibular nerve enters the mandible (mandibular lingula), mesial buccal cusp of the first molar (lower molar), mesial edge of the lower central incisor (lower central incisor), the most protruding part of the mandibular (pogonion), the posterior portion of the mandible where the angle of the mandible changes when viewed from the side (gonion) and top of mandibular head (condylion; Fig. 2). A single orthodontist set all measurement points, which are anatomically highly reproducible and pre-known to have an extremely small measurement error.[9,16,17]

Definition of 3D Coordinates

Each point is represented numerically as 3D coordinates X, Y, and Z, following the method described by Arizumi et al.[17] (Fig. 3A). X represents left-right differences, with larger values indicating deviation from the origin (Fig. 3B). Y is parallel to the line connecting the midpoint of the most posterior points of the left and right occipital condyles and the most posterior point of the nasion, representing the anterior–posterior position relative to the origin. Positions anterior to the origin are designated as positive (Fig. 3C). Z is parallel to the line connecting the origin with the posterior point of the junction between the lower border of the vomer and the horizontal plate of the palatine bone and perpendicular to the line connecting the origin with the nasion, representing the vertical position relative to the origin (Fig. 3D). Positions below the origin are designated as positive.

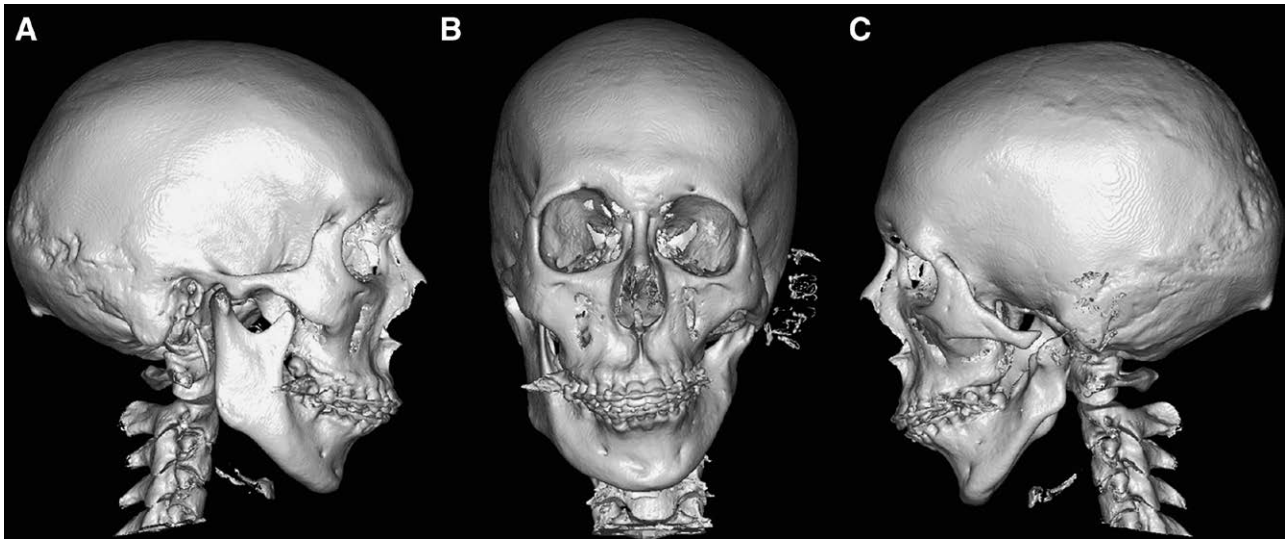

Fig. 1. CT image of the patient diagnosed with hemifacial microsomia (type II). A, The right side is the nonaffected side. B, The middle is the front view. C, The left side is the affected side.

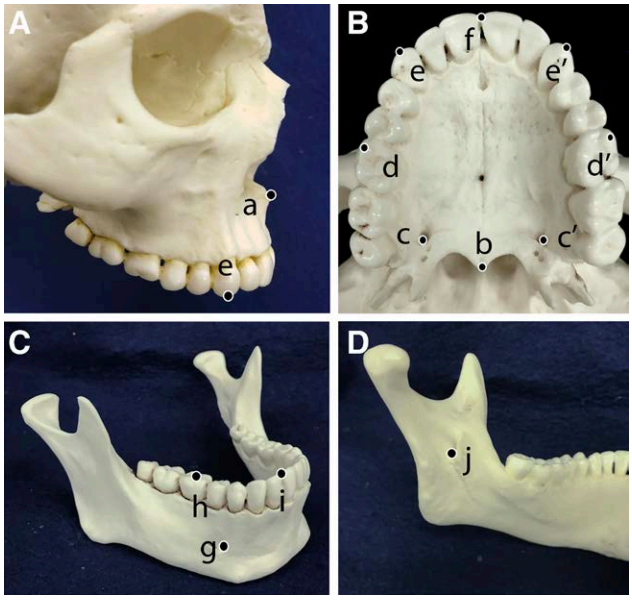

Fig. 2. Measurement points of maxilla and mandible. A, a, ANS. ee′, cusp of maxillary canine. B, b, PNS. cc′, Palatine foramen. dd′, upper molar. ee′, canine. f, Upper central incisor. C, g, Mental foramen. h, lower molar. i, Lower central incisor. D, j, mandibular lingla.

Creation of Treatment Objectives

Using 3D reconstruction software (proplan CMF ver3.1, Materialize Inc.), we performed 3D reconstruction of CT images obtained just presurgery and set treatment objectives through surgical simulations. The treatment objectives were defined by aligning the X coordinates of the ANS, PNS, and upper incisor of the upper jaw at the origin (0, y, z), thus aligning the midlines of the maxilla and mandible with the facial midline. In the lower jaw, the lengths of the mandibular ramus and body were measured, with left-right differences eliminated through bone distraction. With the X coordinate of the lower incisor at the origin, the midlines of the face and mandible were aligned, and the overbite and overjet were set at 2.5 mm to achieve ideal occlusion of the upper/lower molars. Meanwhile, efforts were made to adjust the y and z axes of the canine, upper molar, and lower molar on both the affected and nonaffected sides to achieve maximum left-right symmetry.

Midline Deviation

We conducted a comparison using the established coordinate system to assess the deviations in the presurgery, postsurgery, and treatment objectives groups. The parameters used the measurements of ANS, PNS, upper incisor, and lower incisor relative to the x axis as the reference for the face midline. Based on previous research,[11] these data, despite the small sample size, follow a normal distribution and exhibit homoscedasticity. Therefore, a one-way analysis of variance, a parametric method, was conducted. For multiple comparisons, we used the Dunnett method, with the treatment objectives group as the control.

Regarding Mandibular Bone Distraction

Before the mandible distraction, Le Fort I osteotomy was performed (Fig. 4A), in which the goal was to achieve symmetry by aligning the mandibular bone of the affected side closer to that of the nonaffected side through both horizontal and vertical distraction osteogenesis as the primary bone-cutting. Two bone distraction devices were installed on the affected side (Fig. 4B, C). The measurement sites on the CT 3D reconstructed images included the pogonion-gonion mandibular length and condylion-gonion mandibular height on both the affected and nonaffected sides. For statistical analysis, a paired *t* test was conducted to verify the symmetry of mandibular length and height between the

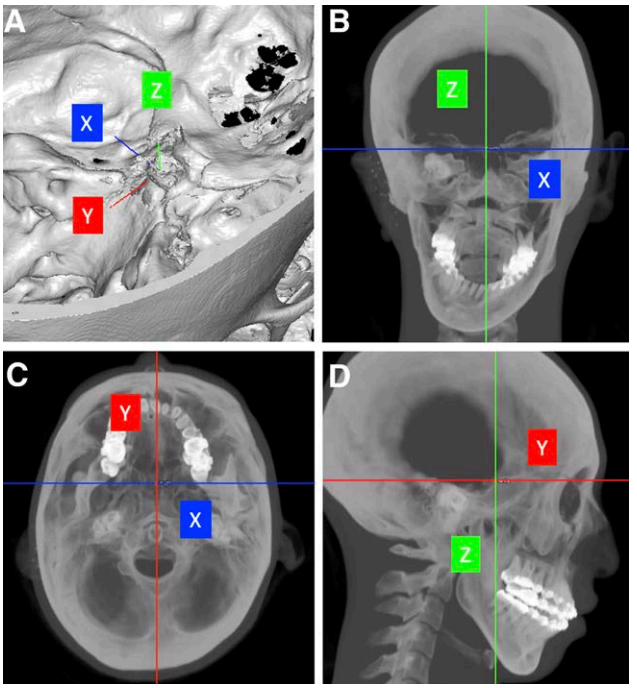

Fig. 3. Coordinate origin and axis. A, The coordinate origin and coordinate axis direction of the coordinate system of this study created in the right-handed system (world coordinate system). B, Coronal image. C, Axial image. D, Sagittal image.

affected and nonaffected sides in both the presurgery and postsurgery groups.

Comparison of Symmetry Using XYZ Coordinates of Each Measurement Point

By comparing the X, Y, and Z coordinates of the affected and nonaffected sides in the presurgery, treatment objectives, and postsurgery groups using the 3D coordinates of each set measurement point, we aim to investigate the factors contributing to facial asymmetry in both the upper/lower jawbones.

Superimposition of 3S Reconstructed Images between Treatment Objectives Group and Postsurgery Group

Areas of significant asymmetry are highlighted by using color variations to represent differences when superimposed on the 3D reconstructed images of the treatment objectives and postsurgery groups at the origin point, which helps reveal regions with noticeable visual asymmetry.

Statistical Analysis

Statistical analysis was performed using the statistical software GraphPad Prism 9 (GraphPad Software Inc. Boston, Ma.). From previous studies,[17] these indices approximate a normal distribution in the population. Therefore, it was appropriate to use a parametric method, with a paired *t* test with affected and nonaffected sides used to account for individual differences. The X coordinate of the mental foramen area on the affected side,

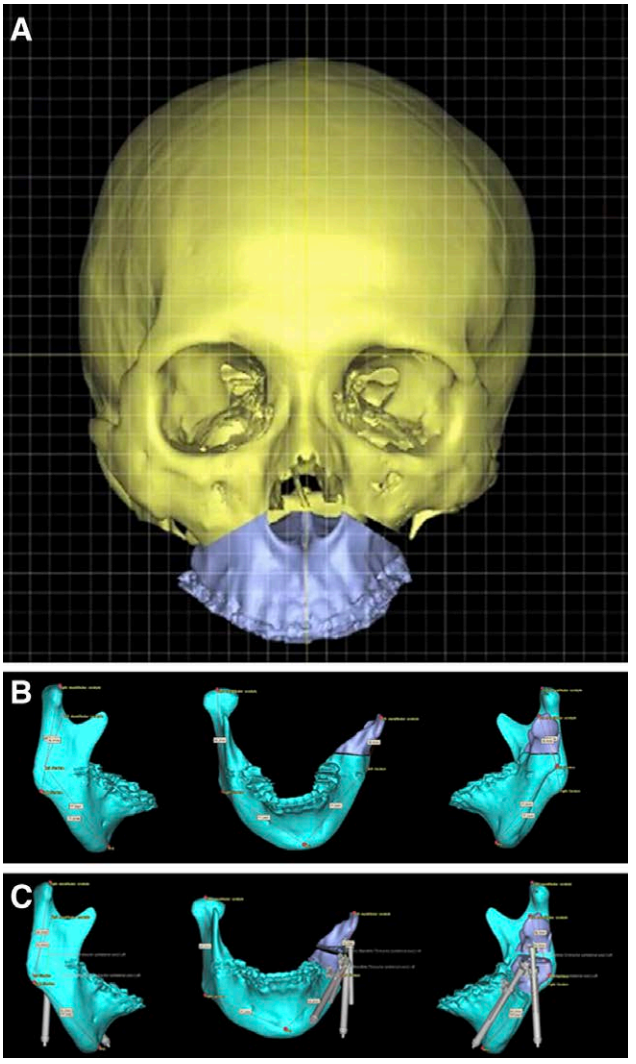

Fig. 4. Simulation of maxillary and mandible surgery. A, Maxillary bone positioning to define the treatment objective, the X coordinates of ANS, PNS, and upper incisor were aligned with the origin (0, y, z) to align the midline of the maxillomandibular bone with the facial midline, and the upper molar, canine coordinates on the z axis were aligned with the nonaffected side so that the occlusal plane becomes the horizontal plane. B, Mandible bone measurements. Mandibular height: Mandibular condylion to Gonion. Mandibular length: Pogonion to Gonion. C, Evaluation after bone distraction.

where patients complained the most, was analyzed using G*Power (https://www.psychologie.hhu.de/arbeitsgruppen/allgemeine-psychologie-und-arbeitspsychologie/gpower.html), and the result was n = 5, which was chosen because of the need to identify the problem area with the fewest number of subjects.

RESULTS

Deviation of Measurement Points from Facial Midline

A three-way comparison was made: the presurgery, treatment objectives, and postsurgery groups, for X, Y, and Z of points ANS, PNS, upper incisor, and lower incisor.

In the X coordinate, significant differences were observed between the presurgery and the treatment objectives groups for all items: ANS ($P = 0.003$), PNS ($P = 0.004$), upper incisor ($P = 0.002$), and lower incisor ($P = 0.044$), with no significant differences found in the X coordinate between the treatment objectives and the postsurgery groups for all items. No significant differences were observed in the Y and Z coordinates for all items among the three groups (Figs. 5 and 6).

Symmetry Through Mandibular Bone Distraction

A comparison of mandibular bone length between the affected and nonaffected sides in the presurgery group revealed a significant difference ($P = 0.007$). Similarly, a significant difference was observed when comparing the affected and nonaffected sides in the postsurgery group ($P = 0.04$). A significant difference in mandibular bone height was found when comparing the affected and nonaffected sides in the presurgery group ($P = 0.005$). Likewise, a significant difference was observed when comparing the affected and nonaffected sides in the postsurgery group ($P = 0.012$; Fig. 7).

Comparison of Affected Side and Nonaffected Side Using 3D Coordinates

In the presurgery group, an examination of the spatial relationship of the 3D coordinates at each measurement point between the affected and nonaffected sides revealed significant differences in all items except for the Y coordinate of the palatine foramen, upper molar, and

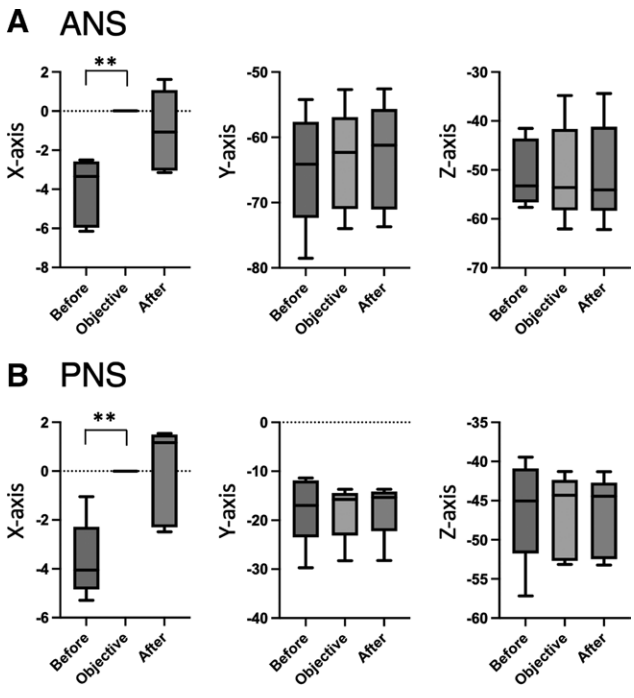

Fig. 5. Comparison of skeletal facial midline against before surgery, treatment objectives, and after surgery. A, Presurgery and postsurgery comparison for ANS treatment objectives. B, Presurgery and postsurgery comparison for PNS treatment objectives. $^{**}P < 0.01$, n = 5.

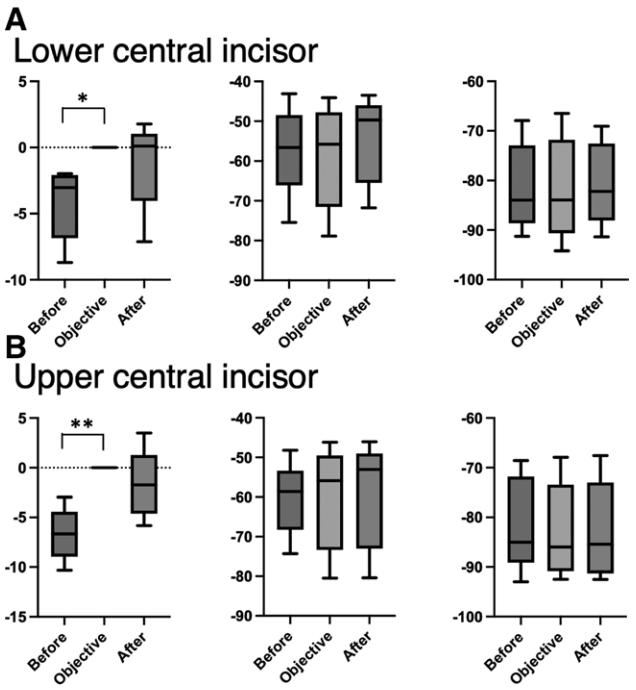

Fig. 6. Comparison of mandibular length and height between affected side and nonaffected side before and after surgery. A, Presurgery and postsurgery comparison for ANS treatment objectives. B, Presurgery and postsurgery comparison for PNS treatment objectives. $^{*}P < 0.05$, $^{**}P < 0.01$, n = 5.

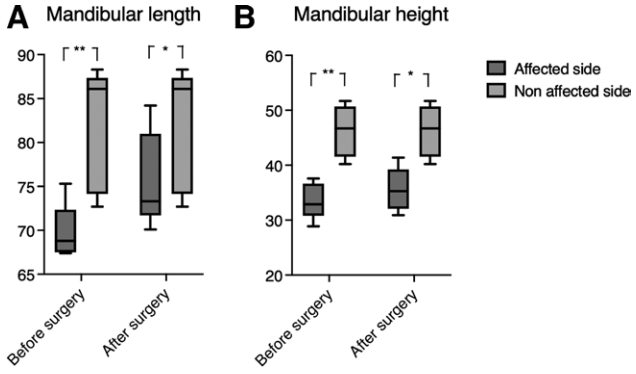

Fig. 7. Before surgery, treatment objectives, and after surgery position of the upper and lower anterior teeth in the midline of the face. A, Mandibular length comparison between the affected and nonaffected sides before and after surgery. B, Mandibular height comparison between the affected and nonaffected sides before and after surgery. $^{*}P < 0.05$, $^{**}P < 0.01$, n = 5.

canine (Table 1). In the treatment objectives group, the same examination showed no significant differences in any X, Y, and Z (Table 2). With these treatment objectives, an examination was conducted in the postsurgery group, where Le Fort I osteotomy of the maxilla and mandibular bone elongation were performed. Results showed no significant differences in all items in terms of X coordinate. However, a significant difference was observed for Y in the mental foramen ($P = 0.039$). Significant differences for Z

Table 1. Comparison of Symmetry of 3D Coordinates at Each Measurement Point on the Affected and Nonaffected Side in before Surgery

	Affected Side		Nonaffected Side					
Before Surgery	Average	SD	Average	SD	Mean of Differences	95% CI	*P*	
Palatine foramen_X	12.23	2.22	14.08	2.33	6.44	1.65–11.23	0.02	*
Upper molar_X	25.35	2.39	26.51	3.43	7.39	1.59–13.19	0.02	*
Canine_X	14.14	4.00	25.01	1.70	10.87	5.36–16.38	>0.01	**
Lower molar_X	25.10	7.62	28.56	8.71	5.47	0.27–10.66	0.04	*
Mandibular lingula_X	37.69	3.29	43.96	2.57	6.26	0.85–11.68	0.03	*
Mental foramen_X	16.01	4.07	27.97	3.86	11.95	3.61–20.30	0.02	*
Palatine foramen_Y	24.06	7.77	26.51	8.16	2.45	-0.43 to 5.32	0.08	N. S.
Upper molar_Y	30.60	9.86	38.37	9.03	7.77	2.68–12.86	0.08	N. S.
Canine_Y	49.27	7.54	52.18	8.31	2.91	–1.80 to 7.62	0.16	N. S.
Lower molar_Y	30.69	9.11	36.53	9.64	6.18	0.29–12.07	0.04	*
Mandibular lingula_Y	–3.66	9.24	– 0.69	9.61	4.67	1.34–8.00	0.02	*
Mental foramen_Y	28.88	9.80	34.42	10.34	5.54	0.45–10.63	0.04	*
Palatine foramen_Z	45.30	6.38	48.70	7.91	3.40	0.65–6.15	0.03	*
Upper molar_Z	69.02	8.13	74.60	8.34	5.58	2.49–8.67	0.01>	**
Canine_Z	75.60	8.07	81.83	9.52	6.23	3.77–9.10	0.01>	**
Lower molar_Z	69.53	7.72	76.18	9.73	6.65	3.76–9.54	0.01>	**
Mandibular lingula_Z	46.21	6.70	54.98	7.30	8.77	2.40–15.14	0.02	*
Mental foramen_Z	87.71	11.19	97.73	10.59	10.01	4.55–15.48	0.01>	**

Table 2. Comparison of Symmetry of 3D Coordinates at Each Measurement Point on the Affected and Nonaffected Side in Treatment Objectives

	Affected Side		Nonaffected Side					
Treatment Objectives Measurement Item	Average	SD	Average	SD	Mean of Differences	95% CI	*P*	
Palatine foramen_X	15.84	3.65	14.73	4.53	–1.11	–3.64 to 1.42	0.291	NS
Upper molar_X	25.50	4.43	26.47	2.16	0.97	–2.92 to 4.85	0.528	NS
Canine_X	19.66	1.41	19.11	2.45	–0.55	–4.57 to 3.48	0.726	NS
Lower molar_X	23.56	2.69	24.57	3.98	1.01	–3.08 to 5.09	0.531	NS
Mandibular lingula_X	41.97	4.21	39.81	7.45	–2.16	–11.83 to 7.51	0.569	NS
Mental foramen_X	21.71	4.67	23.46	2.36	1.75	–6.33 to 9.83	0.58	NS
Palatine foramen_Y	26.37	7.43	25.53	6.72	–0.84	–2.42 to 0.73	0.211	NS
Upper molar_Y	38.26	9.86	35.62	10.24	–2.64	–5.96 to 0.68	0.092	NS
Canine_Y	51.51	10.69	51.15	11.92	–0.35	–3.14 to 2.43	0.744	NS
Lower molar_Y	31.65	12.00	30.59	12.51	–1.07	–5.17 to 3.04	0.511	NS
Mandibular lingula_Y	-4.21	6.94	-5.37	4.51	–1.17	–4.71 to 2.38	0.413	NS
Mental foramen_Y	31.80	15.75	25.91	16.55	–5.89	–4.71 to 2.38	0.115	NS
Palatine foramen_Z	49.78	6.96	50.07	6.24	0.29	–1.32 to 1.90	0.643	NS
Upper molar_Z	71.56	6.46	73.55	6.87	1.99	–1.32 to 1.90	0.331	NS
Canine_Z	77.41	8.39	79.92	9.53	2.51	–1.13 to 6.15	0.128	NS
Lower molar_Z	71.92	8.39	72.14	8.29	0.22	–0.52 to 0.97	0.452	NS
Mandibular lingula_Z	51.84	9.73	51.13	10.48	–0.71	–11.72 to 10.30	0.867	NS
Mental foramen_Z	96.21	6.62	96.13	8.54	–0.08	–4.11 to 3.95	0.957	NS

were found in the canine ($P = 0.036$) and mental foramen ($P = 0.047$; Table 3).

Superimposition of 3D Constructed Images between Treatment Objectives and After Surgery

In the representative case, the treatment results and objectives were demonstrated via superimposition with Sella set as the origin point. The color-coding indicates that a difference of 6.0 mm or less for purple, 6.0–3.0 mm for red, and 3.0 mm or less for yellow. The most significant differences, marked in purple, were observed near the mental foramen on the affected side, corresponding to the region where significant differences were observed when comparing the affected and nonaffected sides postsurgery (Fig. 8).

DISCUSSION

HFM incidence varies widely in reports, ranging from 3000 to 26,000 individuals with an estimated occurrence of one.[1,3,15,18,19] No significant gender difference exists, with a male-to-female ratio of 1.09:1.[20] Although HFM is a common congenital anomaly, treatment approaches vary widely. With limited cases involving the surgical technique we devised,[14] our study included only five cases of HFM type II (three men and two women). In our plastic surgery

Table 3. Comparison of Symmetry of 3D Coordinates at Each Measurement Point on the Affected and Nonaffected Side in after Surgery

After Surgery Measurement Item	Affected Side	Nonaffected Side	Mean of Differences	95% CI		*P*	
After Surgery Measurement Item	Average		SD		Average	SD	*P*	
Palatine foramen_X	15.55	3.99	1369	316	−186	−672 to 301	035	NS
Upper molar_X	26.55	3.00	2583	176	−071	−649 to 506	075	NS
Canine_X	21.87	2.88	1627	381	−559	−1241 to 123	009	NS
Lower molar_X	26.14	4.36	2397	402	−217	−973 to 540	047	NS
Mandibular lingula_X	40.16	2.34	3861	924	−155	−1507 to 1198	077	NS
Mental foramen_X	13.16	8.79	633	668	−301	−869 to 267	022	NS
Palatine foramen_Y	25.19	6.19	2542	598	024	−273 to 320	083	NS
Upper molar_Y	35.18	10.82	3722	846	204	−501 to 909	047	NS
Canine_Y	50.67	13.18	5056	916	−011	−496 to 473	095	NS
Lower molar_Y	30.53	8.48	3053	668	000	−479 to 480	100	NS
Mandibular lingula_Y	-6.37	5.65	−599	262	037	−805 to 879	091	NS
Mental foramen_Y	23.66	14.31	3014	1053	648	052 to 1244	004	*
Palatine foramen_Z	48.93	7.73	5072	574	179	−163 to 520	022	NS
Upper molar_Z	72.05	11.97	7614	867	409	−158 to 977	012	NS
Canine_Z	76.44	9.84	8070	859	426	045 to 808	004	*
Lower molar_Z	71.71	11.70	7582	915	411	−100 to 922	009	NS
Mandibular lingula_Z	51.28	10.63	5746	1019	618	−093 to 1329	007	NS
Mental foramen_Z	95.46	9.66	10229	1380	682	014 to 1351	005>	*

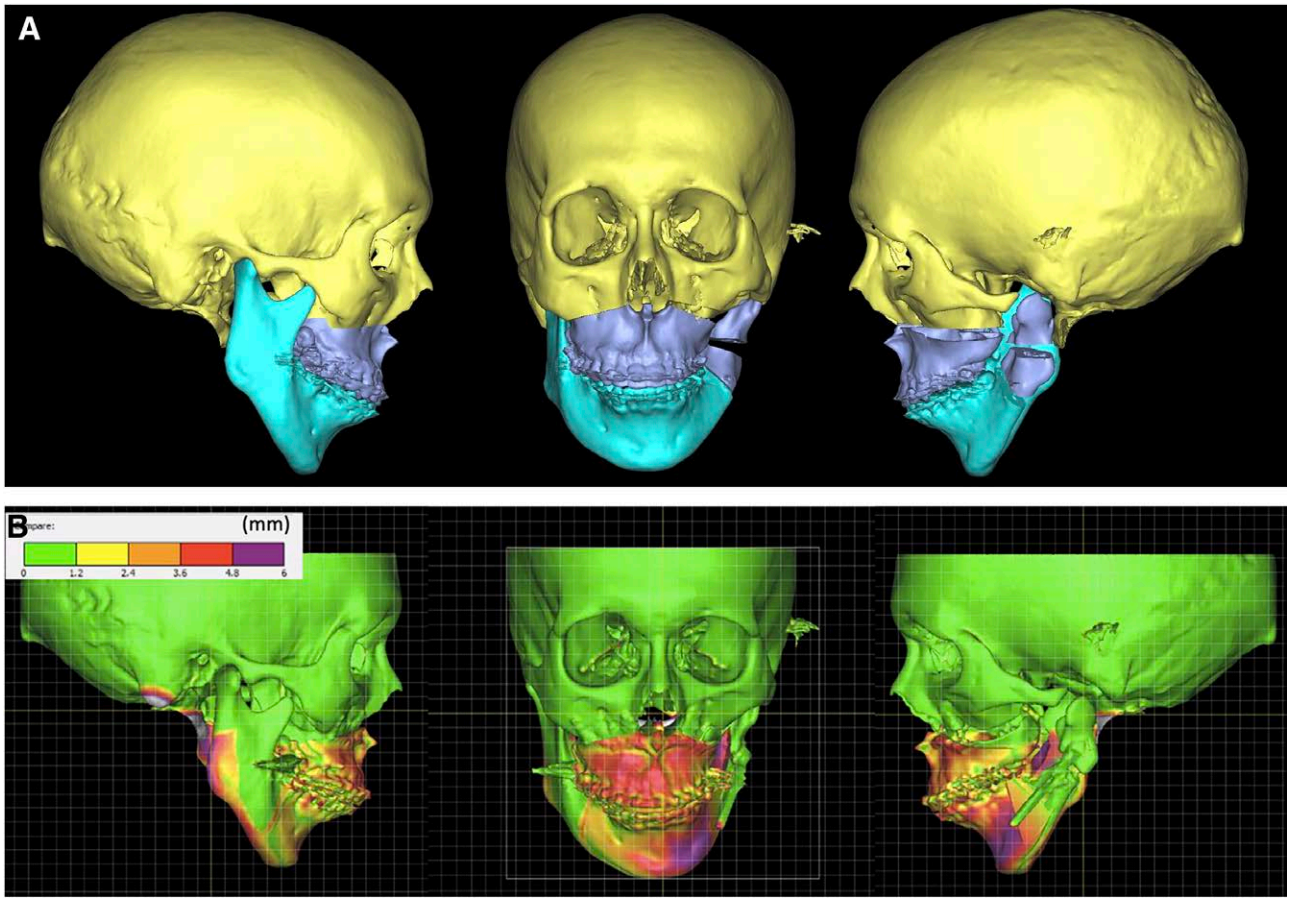

Fig. 8. Visual treatment objectives and evaluation of actual treatment results. A, Completion drawing of treatment objective. B, Superimposition of the actual treatment result and the treatment objectives.

department, for type I and type IIA cases, simultaneous upper/lower jaw surgery using Le Fort I osteotomy is feasible. For type III cases, upper/lower jaw surgery is performed, with lower jaw osteotomy on the nonaffected side. For type IIB, treatment objectives are simulated presurgery to set the lower jawbone distraction for facial symmetry.

HFM often exhibits significant asymmetry, as patients undergo upper/lower jaw osteotomy to improve malocclusion and facial appearance.[21] Conventional two-dimensional evaluations make it difficult to measure and assess the differences in the left-right movement, which involves rotation of the upper/lower jaws. As mentioned, this condition is characterized by hard and soft tissue malformation in the ear region,[7,22] lowering the reproducibility of frontal and lateral cephalograms. With 3D CT data models, simulating preoperative bone-cutting designs and the movement and direction of bone fragments is now possible. However, evaluations for preoperative and postoperative changes and asymmetry degree in HFM have only reported two-dimensional assessments including distance measurements.[22–26] Therefore, we utilized stable landmark coordinates with a fixed origin (X, Y, Z = 0, 0, 0) unaffected by craniofacial deformations for a 3D positional evaluation.[17]

The objectives created were based on each measurement coordinate to achieve symmetry. When planning for conditions of facial asymmetry, methods such as reversing the nonaffected side from the midline to assess symmetry[27] or measuring distances from a set midline for each measurement point[28] have been reported. However, for this condition, challenges exist in determining the midline due to abnormalities in the formation and positioning of the zygomatic arch and external auditory canal traditionally been used as horizontal references. Therefore, we chose a method to establish a coordinate system[17] by setting reference points inside the cranial cavity and evaluating the coordinate values.

Comparing the affected side and nonaffected sides presurgery, significant left-right differences were observed in all X, Y, and Z items. For the X horizontal position, all items of the upper/lower jaw on the nonaffected side have seemingly moved toward the affected side. For the Y anterior–posterior position, the values on the affected side were smaller in all items, suggesting that the affected side was further back than the nonaffected side. For the Z vertical position, the values on the affected side were smaller in all measurement items, suggesting that the affected side was higher than the nonaffected side.

At the presurgery stage, it became clear that the affected side had not only horizontal deviation but also anterior–posterior and horizontal deviations. When setting the treatment objectives, it was established to achieve 3D symmetry in all dimensions, horizontal (X coordinate), anterior–posterior (Y coordinate), and vertical (Z coordinate), confirmed through the comparison between the affected and nonaffected sides in the treatment objectives. Procedures were performed based on them, including Le Fort I osteotomy on the maxilla and vertical and horizontal osteotomies on the mandible for facial symmetry through bone distraction.

Comparing the affected and nonaffected sides in postsurgery, horizontal symmetry in the jaw and face was achieved. However, in the mental foramen area, the affected side was positioned posteriorly compared with the nonaffected side in the anterior–posterior direction. In terms of vertical position, the canine and mental foramen on the affected side were located above the nonaffected side. To understand these findings, a comparison of mandibular length and height between the affected and nonaffected sides before and after bone distraction was conducted, which showed that the significant differences observed presurgery were not improved postsurgery.

In our approach, we prioritize the positioning of the maxilla and fix it in alignment with the treatment objectives using Le Fort I osteotomy before mandibular bone distraction.[14] When the 3D positions of the affected and nonaffected sides in the maxilla are symmetrical postsurgery, the challenge lies in achieving sufficient vertical elongation of the mandibular ramus and horizontal elongation of the mandibular body with the mandibular distraction device. Precisely controlling the 3D direction is challenging.[28–30] In other words, there is an issue with setting the mandibular elongation. Orthodontically, achieving a tight occlusion of the upper/lower dental arches is crucial; with a skeletal-dominant configuration, instability in the occlusion may exists. It is important to pay attention to the movement position of the canine teeth on the affected side.

The position of the mandibular head on the affected side is expected to be different between the 3D reconstruction image using CT presurgery due to the malformation and the position postsurgery, hence setting the mandibular elongation is important. However, estimating the position of the mandibular head postsurgery is difficult[30] as a future task. HFM type IIB has an unstable relationship between the condyle and the glenoid fossa and a less than ideal amount of movement of the affected side relative to the treatment objectives, requiring consideration of the bone distraction amount.

From the superimposition of representative CT 3D reconstructed images of treatment objectives and postsurgery, insufficient volume exists in the mental foramen area, similar to the results of 3D coordinate measurements. Therefore, adjustments to the mandibular elongation device, augmentation through implants or fat injection, or shaving of the corresponding area on the nonaffected side may be considered potential solutions.[31,32]

In clinical application, it is crucial to first set the treatment objectives using the 3D reconstructed images obtained by CT presurgery. Special attention should be paid to the vertical and anterior–posterior relationships near the mental foramen on the affected side. Although this study was limited by the small number of cases, we will report on the surgical method that can increase the number of cases and obtain facial symmetry using an improved method based on the results.

CONCLUSIONS

The site-specific evaluation using 3D coordinate measurements in HFM has revealed that relying solely on a frontal view judgment is insufficient for facial symmetry,

requiring improvements in the anterior–posterior and vertical dimensions near the mental foramen on the affected side. Setting individualized treatment objectives for each patient is essential, including innovative approaches to mandibular bone distraction with additional augmentation procedures.

Takenobu Ishii, DDS, PhD
Department of Orthodontics
Tokyo Dental College, Chiba Dental Centre
1-2-2, Masago, Mihama-ku
Chiba, Japan. 261-8502
E-mail: ishiit@tdc.ac.jp

DISCLOSURE

The authors have no financial interest to declare in relation to the content of this article.

ACKNOWLEDGMENTS

This research was conducted with the cooperation of the Department of Orthodontics at Tokyo Dental College and the Department of Plastic and Reconstructive Surgery at Keio University School of Medicine. The authors would like to express their gratitude for these collaborations.

REFERENCES

1. Grabb WC. The first and second branchial arch syndrome. *Plast Reconstr Surg.* 1965;36:485–508.
2. Murray JE, Kaban LB, Mulliken JB. Analysis and treatment of Hemifacial microsomia. *Plast Reconstr Surg.* 1984;74:186–199.
3. Paul MA, Opyrchał J, Knakiewicz M, et al. Hemifacial microsomia review: recent advancements in understanding the disease. *J Craniofac Surg.* 2020;31:2123–2127.
4. McCarthy JG, Stelniki EJ, Grayson BH. Distraction osteogeneis of the mandible: a ten-year experience. *Semin Orthod.* 1999;5:3–8.
5. Hofrath H. Die Bedeutumg von Roentgenfern und Abst and saufnahme fuer die Diagnostik von Kieferanomalien. *Fortschr Orthodont.* 1931;1:232–236.
6. Broadbent BH. A new technique and its application to orthodontics. *Angle Orthod.* 1931;1:45–66.
7. Mafee MF, Schild JA, Kumar A, et al. Radiographic features of the ear-related developmental anomalies in patients with mandibulo facial dysostosis. *Int J Pediatr Otorhinolaryngol.* 1984;7:229–238.
8. Chen YF, Vinayahalingam S, Bergé S, et al. Three-dimensional analysis of the condylar hypoplasia and facial asymmetry in craniofacial microsomia using cone-beam computed tomography. *J Oral Maxillofac Surg.* 2021;79:1750.e1–1750.e10.
9. Liberton DK, Verma P, Contratto A, et al. Development and validation of novel three-dimensional craniofacial landmarks on cone-beam computed tomography scans. *J Craniofac Surg.* 2019;30:e611–e615.
10. Liu K, Xu Y, Abdelrehem A, et al. Application of virtual planning for three-dimensional guided maxillofacial reconstruction of Pruzansky-Kaban III hemifacial microsomia using custom made fixation plate. *J Craniofac Surg.* 2021;32:896–901.
11. Tan A, Chai Y, Mooi W, et al. Computer-assisted surgery in therapeutic strategy distraction osteogenesis of hemifacial microsomia: accuracy and predictability. *J Craniomaxillofac Surg.* 2019;47:204–218.
12. Kim BC, Bertin H, Kim HJ, et al. Structural comparison of hemifacial microsomia mandible in different age groups by three-dimensional skeletal unit analysis. *J Craniomaxillofac Surg.* 2018;46:1875–1882.
13. Wang P, Zhang Z, Wang Y, et al. The accuracy of virtual-surgical-planning-assisted treatment of hemifacial microsomia in adult patients: distraction osteogenesis vs. orthognathic surgery. *Int J Oral Maxillofac Surg.* 2019;48:341–346.
14. Nakajima H, Sakamoto Y, Tamada I, et al. Maxillary driven simultaneous maxilla mandibular distraction for hemifacial microsomia. *J Craniomaxillofac Surg.* 2011;39:549–553.
15. Pruzansky S. Not all dwarfed mandibles are alike. *Birth Defects Orig Artic Ser.* 1969;5:120–129.
16. Ono I, Ohura T, Narumi E, et al. Three-dimensional analysis of craniofacial bones using three-dimensional computer tomography. *J Craniomaxillofac Surg.* 1992;20:49–60.
17. Ariizumi D, Sakamoto T, Ishii T, et al. Three-dimensional coordinate system for hemifacial microsomia. *Plast Reconstr Surg Glob Open.* 2020;8:e2761.
18. Rooijers W, Tio PAE, van der Schroeff MP, et al. Hearing impairment and ear anomalies in craniofacial microsomia: a systematic review. *Int J Oral Maxillofac Surg.* 2022;51:1296–1304.
19. Rollnick BR, Kaye CI, Nagatoshi K, et al. Oculoauriculovertebral dysplasia and variants: phenotypic characteristics of 294 patients. *Am J Med Genet.* 1987;26:361–375.
20. Xu S, Zhang Z, Tang X, et al. The influence of gender and laterality on the incidence of hemifacial microsomia. *J Craniofac Surg.* 2015;26:384–387.
21. Ogata H, Sakamoto Y, Sakamoto T, et al. Maxillomandibular tandem osteotomy with distraction osteogenesis for hemifacial microsomia. *J Craniofac Surg.* 2012;23:1362–1363.
22. Gougoutas AJ, Singh DJ, Low DW, et al. Hemifacial microsomia: clinical features and pictographic representations of the OMENS classification system. *Plast Reconstr Surg.* 2007;120:112e–113e.
23. Zhang Z, Li X, Chen X, et al. Correlations between mandible condylar structures and external ear deformities in hemifacial microsomia with three-dimensional analysis. *J Craniofac Surg.* 2022;33:1154–1158.
24. Yamada A, Ueda K, Yorozuya-Shibazaki R. External ear reconstruction in hemifacial microsomia. *J Craniofac Surg.* 2009;20(Suppl 2):1787–1793.
25. Cevidanes LH, Bailey LJ, Tucker SF, et al. Three dimensional cone- beam computed tomography for assessment of mandibular changes after orthognathic surgery. *Am J Orthod Dentofacial Orthop.* 2007;131:44–50.
26. Takahashi-Ichikawa N, Susami T, Nagahama K, et al. Evaluation of mandibular hypoplasia in patients with hemifacial microsomia: a comparison between panoramic radiography and three-dimensional computed tomography. *Cleft Palate Craniofac J.* 2013;50:381–387.
27. Yoshida S, Suga K, Nakano Y, et al. Postoperative evaluation of grafted bone in alveolar cleft three dimensional computed tomography data. *Cleft Palate Craniofac J.* 2013;50:671–677.
28. Yáñez-Vico RM, Iglesias-Linares A, Torres-Lagares D, et al. A new three-dimensional analysis of asymmetry for patients with craniofacial syndromes. *Oral Dis.* 2013;19:755–762.
29. Meazzini MC, Mazzoleni F, Gabriele C, et al. Mandibular distraction osteogenesis in hemifacial microsomia: long-term follow-up. *J Craniomaxillofac Surg.* 2005;33:370–376.
30. Paeng JY, Lee JH, Lee JH, et al. Condyle as the point of rotation for 3-D planning of distraction osteogenesis for hemifacial microsomia. *J Craniomaxillofac Surg.* 2007;35:91–102.
31. Sinclair N, Gharb BB, Papay F, et al. Soft tissue reconstruction in patients with hemifacial microsomia: a systematic review of the literature. *J Craniofac Surg.* 2019;30:879–887.
32. Igelbrink S, Zanettini LMS, Bohner L, et al. Three-dimensional planning of the mandibular margin in hemifacial microsomia using a printed patient-specific implant. *J Craniofac Surg.* 2020;31:2297–2301.